

# RSC Advances



This is an *Accepted Manuscript*, which has been through the Royal Society of Chemistry peer review process and has been accepted for publication.

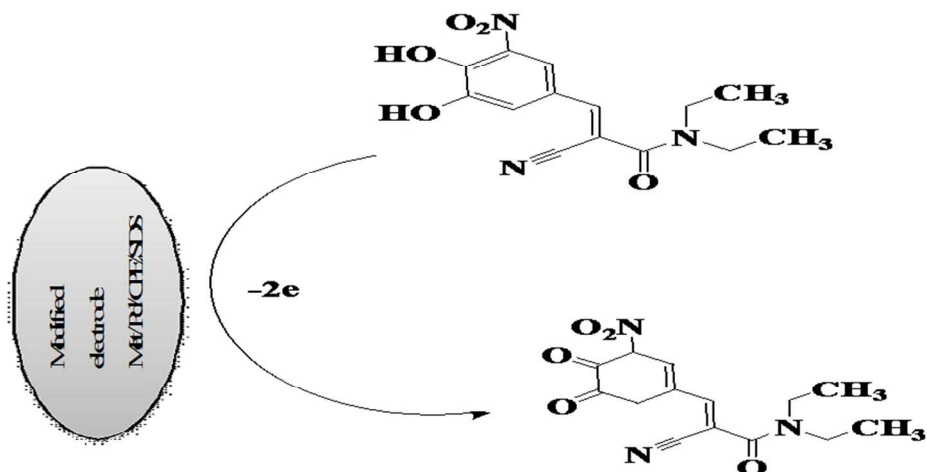
*Accepted Manuscripts* are published online shortly after acceptance, before technical editing, formatting and proof reading. Using this free service, authors can make their results available to the community, in citable form, before we publish the edited article. This *Accepted Manuscript* will be replaced by the edited, formatted and paginated article as soon as this is available.

You can find more information about *Accepted Manuscripts* in the [Information for Authors](#).

Please note that technical editing may introduce minor changes to the text and/or graphics, which may alter content. The journal's standard [Terms & Conditions](#) and the [Ethical guidelines](#) still apply. In no event shall the Royal Society of Chemistry be held responsible for any errors or omissions in this *Accepted Manuscript* or any consequences arising from the use of any information it contains.

A novel methionine/palladium nanoparticles modified carbon paste electrode in a micellar medium for simultaneous determination of three antiparkinsonism drugs

Nahla N. Salama<sup>a</sup>, Shereen M. Azaba, Mona A. Mohamed<sup>a\*</sup>, Amany M. Fekryb



Scheme 1: The suggested oxidation mechanism of EN at Met/Pd/CPE/SDS

254x190mm (96 x 96 DPI)

## A novel methionine/palladium nanoparticles modified carbon paste electrode for simultaneous determination of three antiparkinsonism drugs

Nahla N. Salama<sup>a</sup>, Shereen M. Azab<sup>a</sup>, Mona A. Mohamed<sup>a\*</sup>, Amany M. Fekry<sup>b</sup>

<sup>a</sup> Pharmaceutical Chemistry Dept., National Organization for Drug Control and Research [NODCAR], 6 Abu Hazem Street, Pyramids Ave, P.O. Box 29, Giza, Egypt

<sup>b</sup> Chemistry Department, Faculty of Science, Cairo University, Giza-12613, Egypt.

---

### Abstract

A simple, novel and reproducible method for separation and simultaneous determination of entacapone (EN), levodopa (LD) and carbidopa (CD) based on methionine/palladium nanoparticles modified carbon paste electrode (Met/Pd/CPE) prepared via the electrodeposition of palladium on methionine/carbon paste modified electrode. Cyclic voltammetry (CV), differential pulse voltammetry (DPV), chronoamperometry (CA), and electrochemical impedance spectroscopy (EIS) techniques were used to characterize the properties of the sensor. Under optimum experimental conditions, the respective linear calibration range was rectilinear over the range from  $2.0 \times 10^{-8}$  to  $0.8 \times 10^{-3}$  mol L<sup>-1</sup> with a correlation coefficient of 0.9997 for differential pulse voltammetry (DPV) in Britton Robinson buffer at pH 2.0. The lower limit of detection (LOD) and limit of quantification (LOQ) were found to be  $7.077 \times 10^{-10}$  mol L<sup>-1</sup> and  $2.35 \times 10^{-9}$  mol L<sup>-1</sup>, respectively. The utility of this modified electrode was demonstrated for the determination of EN in real samples.

**Keywords:** Entacapone; Palladium nanoparticles; Methionine; Modified Carbon paste electrode.

\*E-mail: [salama\\_nahla2004@hotmail.com](mailto:salama_nahla2004@hotmail.com)

National Organization for Drug Control and Research (NODCAR)

6 Abou Hazem Street, Pyramids Ave, P.O. Box 29, Cairo, Egypt

Tel: 202-35851299 , Fax: 202-35855582

## 1. Introduction

Entacapone (EN) is a catechol-O-methyltransferase (COMT) inhibitor recently approved in the European Union as an adjunct to standard preparations of levodopa/benserazide and levodopa/carbidopa for use in patients with Parkinson's disease and end-of-dose motor fluctuations, who can not be stabilized on those combinations (Scheme 1). It has been suggested that the beneficial action of adding EN to this standard therapy is based on enhanced bioavailability of LD<sup>1</sup>. EN is a member of the class of drugs known as nitrocatechols. Pharmacologically, EN converts L-DOPA into a compound that cannot cross the blood brain barrier<sup>2</sup>. EN increases the bioavailability of LD by 5-10% more from standard LD/benserazide preparations than from standard LD/CD preparations.

### Scheme 1

Various analytical methods have been used for EN determination such as spectrophotometric methods<sup>3,4</sup>, HPLC<sup>5-8</sup>, micellar capillary chromatography<sup>9,10</sup> and differential pulse polarographic methods<sup>11,12</sup>. Although above mentioned techniques offer a high degree of specificity, yet, sample preparation and instrumentation limitations preclude their use in routine analysis. Long analysis time, the use of organic solvents and high costs are some of the drawbacks associated with these techniques. Voltammetry is considered as an important electrochemical technique utilized in electroanalytical chemistry. Chemical modified electrodes (CME) have been largely used in the area of electrochemical and biological fields<sup>13-16</sup>.

L-methionine (Met) is one of the two sulfur-containing proteinogenic amino acids with an important role in biological methylation reaction. Whereas most of the efforts have been done on its determination, it also could be electrochemically polymerized

at the surface of an electrode for its modification <sup>17</sup>. The presence of CH<sub>3</sub>SCH<sub>2</sub>-group causes that methionine easily attaches to the electrode surfaces through sulphur atom and creates self-assembled monolayer at these supports <sup>18</sup>. The arrangement of amino acids adlayer is governed by a variety of intermolecular interactions that could occur between carboxylic and amine groups (Coulombic forces and hydrogen bonds) <sup>19</sup>. Recently, the development of biocompatible nanomaterials has opened up a new direction in the development of third-generation biosensors based on direct electron transfer between the drug and the electrode <sup>20</sup>. There is agreement that noble metals such as Pd are initially good catalysts for the electro-oxidation of small organic molecules. Noble metal nanocrystals play an important role in different fields of science, such as catalysis, medicine, electronics, etc. because of their strong redox catalytic activities. Metal nanoparticles have been used in the fabrication of sensors as nanocomposites or when covalently bonded with CNTs <sup>21-23</sup>. Pd nanoparticles are preferable to platinum or gold due to their lower price.

Surfactants have been widely used in chemistry and in particular affecting several electrochemical processes to change the electrical properties of the electrode solution interface and the electrochemical process through adsorption at interfaces or aggregation into supramolecular structures <sup>24</sup>. Several applications of surfactants in electrochemistry are in electroplating <sup>25</sup>, corrosion <sup>26</sup>, electrocatalysis <sup>27</sup>, and electroanalysis <sup>28, 29</sup>.

The simultaneous pharmaceutical analysis of multi-component drugs represents a challenge due to a large total number of analytes present in the sample. These analytes are not only the active pharmaceutical ingredients, but also the impurities that might follow the active substances. A few analytical methods for the

determination of active compounds (EN, LD and CD) in combined tablets are reported: RP-HPLC with UV detection<sup>30</sup>, RP-HPTLC<sup>31</sup> and HPLC<sup>32</sup>.

The objective of this work is to develop Met–palladium nanoparticles modified carbon paste electrode (Met/Pd/CPE). This modified electrode was examined for the first time for determination of EN either alone or in combination with LD and CD, which formulated with EN in Stalevo<sup>®</sup> tablets, and for the determination of EN in pharmaceutical and biological compounds.

## 2. Experimental

### 2.1. Materials and reagents

EN was kindly supplied from Novartis Pharmaceutical Co., Egypt, Met and sodium dodecyl sulphate (SDS) were purchased from Aldrich and were used as received, Britton-Robinson buffer (B-R buffer)  $4.0 \times 10^{-2} \text{ mol L}^{-1}$  was prepared by mixing  $\text{H}_3\text{PO}_4$ , acetic acid and boric acid with the appropriate amount of  $0.2 \text{ mol L}^{-1}$  NaOH to obtain the desired pH 2.0 - 9.0. All solutions were prepared from analytical grade chemicals and sterilized Milli-Q deionized water.

#### 2.1.1. Preparation of modified CPE

Carbon paste electrode (CPE) was prepared by mixing graphite powder (3.0 g) and methionine (0.3 mg) with nujol oil in a glassy mortar. The carbon paste was packed into the hole of the electrode body and smoothed on a filter paper until its shiny appearance. Then the modified electrode was immersed into  $2.5 \times 10^{-3} \text{ mol L}^{-1}$   $\text{PdCl}_2$  in  $0.1 \text{ mol L}^{-1}$   $\text{HClO}_4$  and then cycled between  $-0.25$  and  $+0.65 \text{ V}$  at a scan rate of  $50 \text{ mV s}^{-1}$  for 25 cycles<sup>33</sup> to form Met palladium nanoparticles modified CPE (Met/Pd/CPE). Then  $10 \mu\text{l}$  of  $1 \times 10^{-2} \text{ mol L}^{-1}$  sodium SDS was added to the solution to enhance the peak current.

## 2.2. Instrumental and experimental set-up

### 2.2.1. Electrochemical measurements

All voltammetric measurements were performed using computer-driven, AEW2 Analytical Electrochemical Workstation with ECprog3 electrochemistry software, manufactured by SYCOPEL SCIENTIFIC LIMITED (Tyne & Wear, UK). The one compartment cell with the three electrodes was connected to the electrochemical workstation through a C3-stand from BAS (USA). A platinum wire from BAS (USA) was employed as the auxiliary electrode. All the cell potentials were measured with respect to Ag/AgCl (3 M NaCl) reference electrode from BAS (USA). A Cyberscan 500 digital (EUTECH Instruments, USA) pH-meter with a glass combination electrode served to carry out the pH measurement. All the electrochemical experiments were performed at an ambient temperature of 25 °C. Scanning electron microscopy (SEM) measurements were carried out using a JSM-6700F scanning electron microscope (Japan Electro Company).

### 2.2.2. Impedance spectroscopy measurements

Electrochemical impedance spectroscopy was performed using the electrochemical workstation IM6e Zahner-elektrik, GmbH, (Kronach, Germany). The impedance diagrams were recorded at the peak potential by applying a 10 mV sinusoidal potential through a frequency domain from 100 kHz down to 100 mHz.

## 2.3. Application to human urine

EN urine samples were prepared using a similar method, as reported in Ref<sup>34</sup>. A master solution of  $1 \times 10^{-2}$  mol L<sup>-1</sup> of EN was prepared in methanol. Blank urine samples were collected from 12 subjects, which were then used to prepare urine standards for the method validation. Urine standards were prepared by mixing 500 mL of the  $1 \times 10^{-2}$  mol L<sup>-1</sup> stock with 5000 ml of blank urine to produce a concentration

of  $9.09 \times 10^{-4} \text{ mol L}^{-1}$ . DPVs were recorded according to the recommended procedure for EN. Values of the current (I) versus the corresponding concentration were plotted to obtain the calibration graph. All experiments were performed in compliance with the relevant laws and institutional guidelines, and the institutional committees have approved these experiments.

#### 2.4. Validation in pharmaceutical samples

Commercial pharmaceutical samples containing EN was analyzed to evaluate the validity of the proposed method. Six tablets of Stalevo<sup>®</sup> 200 mg (each tablet contains 200 mg EN, 100 mg LD and 25 mg CD, Novartis pharmaceuticals) were finely powdered and weighed, and the average mass per tablet was determined, and then dissolved in 50 mL methanol and sonicated for 60 min. Then, the solution was filtered into a 25 mL volume calibrated flask, and the residue was washed three times with methanol added to the flask and then diluted to the mark with the same solvent.

#### 2.3. Recommended Experimental procedure

Before any voltammetric measurement, the modified electrode Met/Pd/CPE was cycled between 400 -900 mV with the scan rate of  $100 \text{ mV s}^{-1}$  in  $4.0 \times 10^{-2} \text{ mol L}^{-1}$  Britton–Robinson buffer solution of pH 2 several times until a reproducible response was achieved. Then, the electrode was transferred into another cell containing  $4.0 \times 10^{-2} \text{ mol L}^{-1}$  Britton–Robinson buffer of pH 2 and the proper amount of EN. Then  $10 \mu\text{l}$  of  $1 \times 10^{-2} \text{ mol L}^{-1}$  SDS was added to the solution to enhance the peak current. After accumulating of SDS for 10 s, cyclic voltammograms (CV) were recorded between 400 -900 mV with the scan rate of  $100 \text{ mV s}^{-1}$ .

For DPV procedure, aliquots equivalent  $2.0 \times 10^{-8}$  to  $0.8 \times 10^{-3} \text{ mol L}^{-1}$  EN were transferred into a series of 10-mL volumetric flasks using micro pipette.  $10 \mu\text{L}$  of  $10^{-2} \text{ mol L}^{-1}$  SDS solution were added and the volume was completed to the mark with B-



R buffer pH 2. Quantitatively 5 mL was transferred to the electrolytic cell, and DPV were recorded. The peak current at working Met/Pd/CPE/SDS electrode was measured at scan rate of  $10 \text{ m Vs}^{-1}$  using DPV method.

### 3. Results and discussion

#### 3.1. Morphologies of the different electrodes

The response of the electrochemical sensor was related to its physical morphology. The SEM images of A) CPE, B) Met/CPE and C) Met/Pd/CPE were made, and significant differences in the surface structure were observed. The surface of the CPE was predominated by uniform and smooth shaped graphite flakes and separated layers. On the other hand, the SEM image of Met/CPE shows a thin and compact granular Met film. The electro deposition of palladium nanoparticles gives a random distribution of interstices among the nanoparticles with diameters of 20–50 nm, most of particles homogeneously dispersed on the electrode's surface in the SEM image exhibiting a large surface area.

Insert Fig. 1

#### 3.2. Electrochemistry of EN

The voltammetric behavior of EN was recorded in the range 400 to 900 mV using cyclic voltammetry. Fig. 2 shows typical cyclic voltammograms of  $1.0 \times 10^{-3} \text{ mol L}^{-1}$  EN in B-R buffer pH 2, at scan rate  $100 \text{ mVs}^{-1}$  recorded at four different working electrodes (i.e. bare CPE, Met/CPE, Met/Pd/CPE and Met/Pd/CPE/SDS). For bare CPE the anodic peak current which corresponds to the electrochemical oxidation of EN gives an anodic peak current of  $63 \mu\text{A}$  at 0.627 V. Met was oxidized to free radical at the surface of the electrode the radicals then combined with EN easily causing an enhancement in the peak current to  $91 \mu\text{A}$ . It seems from Fig. 2 that the electrochemical reaction kinetics was improved by Pd nanoparticles

(Met/Pd/CPE) where the anodic peak appears at 0.663 V with a current value of 114.5  $\mu\text{A}$ , which is twice the current observed at bare CPE, this is due to the larger surface area of the modified electrode that improves the electrode kinetics. Addition of SDS to the cell produced a dramatic change in the cyclic voltammograms as the anodic peak current increased to a value of 143.1  $\mu\text{A}$ . Thus, the aggregation of surfactant on the electrode surface makes the electron transfer process take place via the displacement of the adsorbed surfactant by the analyte, the approach of the analyte to the surface of the electrode within the space of one to two head groups of adsorbed surfactant moieties and the formation of ion-pair that anchor onto the surface of the electrode that should possess some hydrophobic character<sup>35</sup>.

Insert Fig. 2

The suggested oxidation mechanism of EN was presented in scheme 1.

Insert scheme 2

### 3.3. Effect of operational parameters

#### 3.3.1. Effect of solution pH

The effect of solution pH on the electrocatalytic oxidation of EN at the Met/Pd/CPE/SDS was studied by the cyclic voltammogram technique using B-R buffers within the pH range of 2–7 (Fig. 3). The anodic peak potentials shifted negatively with the increase in the solution pH, indicating that the electrocatalytic oxidation of EN is a pH-dependent reaction showing that protons have taken part in their electrode reaction processes. The relationship between the anodic peak potential and the solution pH value over the pH range of 2–7 could be fit to the linear regression equation of  $E_{\text{pa}} \text{ (V)} = 8.15 - 0.058 \text{ pH}$ , with a correlation coefficient of  $r = 0.9904$ . The slope was 58.8 mV/pH, which is close to the theoretical value of 59 mV, this indicated that the deprotonation step of EN is prior to the electron transfer step and that the

number of protons and transferred electrons involved in the oxidation mechanism is equal. It was also found that the pH trend was the same for all electrodes (the insert). EN's anodic current responses gave the highest value at pH 2 and at high pH values the current responses were higher than that at low pH values, this is due to the  $pK_a$  value of EN which is 5.68<sup>36</sup>, therefore, EN can be attracted by the negative charges of the electrode.

Insert Fig. 3

### 3.3.2. Effect of scan rate

The effect of different scan rates ( $v$  ranging from 10 to 250  $mVs^{-1}$ ) on the current response of  $1.0 \times 10^{-3} mol L^{-1}$  EN using Met/Pd/CPE/SDS in B-R buffer (pH 2) was studied and a plot of  $i_{pa}$  versus  $v^{1/2}$  gave a straight line relationship up to scan rate 100  $mVs^{-1}$  then deviation occurs (Fig 4). This indicated that the charge transfer was under diffusion control. The inset shows the relation between the anodic peak currents with increasing the scan rate. The oxidation peak currents increased linearly with the linear regression equations as  $i_{pa} (10^{-6} A) = 17.66 v^{1/2} (V s^{-1})^{1/2} - 37.67$  ( $n=5$ ,  $\gamma = 0.9990$ ) suggesting that the reaction is diffusion-controlled electrode reaction.

(Insert Fig 4)

### 3.3.3. Diffusion coefficients of EN

The dependence of the anodic peak current density on the scan rate has been used for the estimation of the “apparent” diffusion coefficient,  $D_{app}$ , for the compounds studied.  $D_{app}$  values were calculated from Randles Sevcik equation<sup>37</sup>

$$i_{pa} = (2.69 \times 10^{-5}) n^{3/2} A C_0^{1/2} D_0^{1/2} v^{1/2} \quad (1)$$

where the constant has units (i.e.  $2.687 \times 10^5 \text{ C mol}^{-1} \text{ V}^{-1/2}$ ).

In these equations:  $i_p$  is the peak current density ( $\text{A cm}^{-2}$ ),  $n$  is the number of electrons appearing in half-reaction for the redox couple,  $v$  is the rate at which the potential is swept ( $\text{V s}^{-1}$ ),  $C_0$  is the analyte concentration ( $1 \times 10^{-6} \text{ mol cm}^{-3}$ ),  $A$  is the electrode area, and  $D$  is the electroactive species diffusion coefficient ( $\text{cm}^2 \text{ s}^{-1}$ ).

The apparent diffusion coefficients,  $D_{\text{app}}$ , of EN in B-R buffer (pH 2) were calculated from cyclic voltammetry (CV) experiments and were found to be  $1.37 \times 10^{-6} \text{ cm}^2 \text{ s}^{-1}$ ,  $2.86 \times 10^{-6} \text{ cm}^2 \text{ s}^{-1}$ ,  $4.27 \times 10^{-6} \text{ cm}^2 \text{ s}^{-1}$  and  $7.08 \times 10^{-6} \text{ cm}^2 \text{ s}^{-1}$  in case of bare CPE, Met/CPE, Met/Pd/CPE and Met/Pd/CPE/SDS, respectively. This indicated the quick mass transfer of the analyte molecules towards Met/Pd/CPE/SDS surface from bulk solutions and/or fast electron transfer process of electrochemical oxidation of the analyte molecule at the electrode-solution interface<sup>16</sup>. Furthermore, it also showed that the redox reaction of the analyte species took place at the surface of the electrode under the control of the diffusion of the molecules from solution to the electrode surface. This marked enhancement of peak current at the surface of the modified electrode confirms that Met, Pd nanoparticles and SDS facilitate the electrochemical reactions.

#### 3.3.4. Chronoamperometric measurements (CA)

Fig. 5 shows the chronoamperometric measurements of EN, performed at a constant applied DC potential on Met/Pd/CPE/SDS in B-R buffer (pH 2) in the current–time profiles obtained by setting the working electrode potential at 690 mV vs. Ag/AgCl for the various concentrations of EN. The inset shows the plots of currents, sampled at fixed time as a function of EN concentration, added to the blank solution at different times after the application of the potential step. For an

electroactive material with the diffusion coefficient ( $D$ ), the current corresponding to the electrochemical reaction (under diffusion control) is described by Cottrell's law<sup>37</sup>:

$$I_{(t)} = nFAC \sqrt{\frac{D}{\pi t}} \quad (2)$$

The level of the Cottrell current, measured for 20 s, increased by increasing EN concentration. The plot of  $I$  versus  $t^{-1/2}$ , showed a straight line (inset) and from its slope, the value of  $D$  could be obtained. According to the Cottrell equation, the slope of fixed time current versus EN concentration plots is  $nFA(D/\pi t)^{1/2}$ , which can provide diffusion coefficient of EN, which was calculated to be  $7.46 \times 10^{-6} \text{ cm}^2 \text{ s}^{-1}$ , which is very close to the value obtained in section 3.3.3.

(Insert Fig 5)

### 3.4. Electrochemical impedance spectroscopy (EIS) studies

In an attempt to clarify the differences among the electrochemical performance of the bare CPE, Met/CPE, Met/Pd/CPE and Met/Pd/CPE/SDS electrochemical impedance spectroscopy (EIS) was employed as a technique for the characterization of each electrode surface. Electrochemical impedance spectroscopy (EIS) is one of the most effective and reliable methods to extract information about electrochemical characteristics of the electrochemical system, including double-layer capacitance, diffusion impedance, determination of the rate of charge transfer and charge transport processes, electrocatalytic systems and solution resistance<sup>38</sup>.

EIS scans of bare CPE, Met/CPE, Met/Pd/CPE and Met/Pd/CPE/SDS are shown in Fig. 6A, B as bode and Nyquist plots, respectively, at potential of 688 mV. The impedance ( $|Z|$ ) and the phase angle maximum ( $\Theta_{\max}$ ) values was found to be in the following order CPE > Met/CPE > Met/Pd/CPE > Met/Pd/CPE/SDS. This means that

CPE electrode has the highest  $|Z|$  and  $\Theta_{\max}$  values. Met/Pd/CPE/SDS has the lowest values of both  $|Z|$  and  $\Theta_{\max}$  value indicating that it is highly conductive of highest observed current as obtained from CV measurements. Nyquist plots (Fig. 6B) show a linear part indicating a diffusion process. Also the diameter of Nyquist plots increases in the following CPE > Met/CPE > Met/Pd/CPE > Met/Pd/CPE/SDS, indicating that the impedance value increases. This means that the highest diffusion process is obtained for Met/Pd/CPE/SDS that confirms well scan rate calculations. The impedance data were thus simulated to the appropriate equivalent circuit for the cases with two time constants for all tested electrodes (inset in Fig. 6A) with 3% error. The model consists of two circuits in series from  $R_1C_1$  and  $Z_wC_2$  parallel combination and both are in series with the solution resistance ( $R_s$ ). In this way  $C_1$  is related to inner layer capacitance and  $C_2$  is related to the inner layer, while  $R_1$  is related to the inner layer resistance<sup>39, 40</sup>. A linear region in the Nyquist plot is related to the diffusion phenomena<sup>39, 41</sup> thereby Warburg component  $Z_w$  is introduced in the model used. This indicates that the mechanism is controlled by diffusion phenomena. Analysis of the experimental spectra were made using Thales software provided with the workstation where the dispersion formula suitable to each model was used<sup>42</sup>. In this complex formula an empirical exponent ( $\alpha = 0$  to 1) is introduced to account for the deviation from the ideal capacitive behavior due to surface in homogenities and adsorption effects<sup>43, 44</sup>. An ideal capacitor corresponds to  $\alpha = 1$  while  $\alpha = 0.5$  becomes the constant phase element in a Warburg component<sup>45</sup>.

Fitting data shows that  $R_1$  and  $Z_w$  values are as following:  $7 \text{ M}\Omega \text{ cm}^2$ ,  $242 \text{ k}\Omega \text{ cm}^2 \text{ s}^{-1/2}$  (CPE),  $1 \text{ M}\Omega \text{ cm}^2$ ,  $534 \text{ k}\Omega \text{ cm}^2 \text{ s}^{-1/2}$  (Met/CPE),  $321 \text{ k}\Omega \text{ cm}^2$ ,  $2645 \text{ k}\Omega \text{ cm}^2 \text{ s}^{-1/2}$  (Met/Pd/CPE) and  $241 \text{ k}\Omega \text{ cm}^2$ ,  $3559 \text{ k}\Omega \text{ cm}^2 \text{ s}^{-1/2}$  for Met/Pd/CPE/SDS. Generally, the data shows that adding Pd and SDS makes the oxidation of EN gives lower impedance

value (highest conductivity) and highest diffusion process and this confirms well SEM images, CV's results and scan rate calculations.

A diffusion phenomena is characterized by  $Z_W$  with a very low frequency slope of -0.5 and will intercept on the log Z axis at  $f = 1$  Hz of  $\sigma\pi^{-1/2}$ , where  $\sigma$  is the Warburg impedance coefficient ( $\text{ohm cm}^2 \text{s}^{-1/2}$ )<sup>46,47</sup>.

$$\log Z = \log \sigma \pi^{-1/2} - \frac{1}{2} \log f \quad (3)$$

$\sigma$  can be obtained from equation (3) by getting log Z values at  $f = 1$  which is 2.782 for Met/Pd/CPE/SDS and are evaluated as 1071.45 which means that diffusion processes take place on the electrode. Diffusion coefficient can be calculated using the following equation<sup>48</sup>:

$$D = \left[ \frac{RT}{\sqrt{2} AF^2 \sigma C} \right]^2 \quad (4)$$

where D is the diffusion coefficient ( $\text{cm}^2 \text{s}^{-1}$ ), A is the area of the electrode ( $\text{cm}^2$ ),  $\sigma$  is Warburg coefficient ( $\text{ohm cm}^2 \text{s}^{-1/2}$ ), C is the concentration of EN ( $\text{mol cm}^{-3}$ ), R is the gas constant,  $\text{J K}^{-1} \text{mol}^{-1}$ , T is the temperature (K) and F is Faraday constant ( $\text{C mol}^{-1}$ ). 3.1522, 2513.0045, 2.9, 1405.96

D is found to be equal  $6.19 \times 10^{-6}$  for Met/Pd/CPE/SDS. Thus diffusion coefficient values calculated from EIS measurements is comparable to that obtained from CV's measurements and confirms it well<sup>39-45</sup>.

### 3.5. Calibration curve

To prove the sensitivity of Met/Pd/CPE/SDS towards the electrochemical measurement of EN, the effect of changing the concentration of EN in B-R buffer pH 2 was studied (Fig. 7). The following are the parameters for the DPV experiments:  $E_i = 400$  mV,  $E_f = 650$  mV, scan rate =  $10 \text{ mV.s}^{-1}$ , pulse width = 25 ms, pulse period =

200 ms, and pulse amplitude = 10 mV. The corresponding calibration plot (inset) was linearly related to EN concentration over the ranges of  $2.0 \times 10^{-8}$  to  $0.8 \times 10^{-3}$  mol L<sup>-1</sup> with a regression equation of  $I_p(\mu\text{A}) = 0.0502 c(\mu\text{mol L}^{-1}) + 0.103$  and a correlation coefficient equals 0.9990.

The linear range for the determination of LD was found to be  $0.50 \times 10^{-5}$  -  $60.00 \times 10^{-3}$  mol L<sup>-1</sup> with a regression equation of  $I_p(\mu\text{A}) = 0.0489c(\mu\text{mol L}^{-1}) + 0.088$ ,  $r = 0.9997$ . The corresponding linear range for the determination of CD was found to be  $0.30 \times 10^{-5}$  -  $15.00 \times 10^{-3}$  mol L<sup>-1</sup> with a regression equation of  $I_p(\mu\text{A}) = 0.0662 c(\mu\text{mol L}^{-1}) + 0.415$ ,  $r = 0.9993$ .

Different batches of the modified Met/Pd/CPE were prepared for the determination of EN and RSD was less than 2%. The limits of detection (LOD) and the limits of quantitation (LOQ) were calculated from the oxidation peak currents of the two linear ranges using the following equations:

$$\text{LOD} = 3s/m$$

$$\text{LOQ} = 10s/m$$

where  $s$  is the standard deviation of the oxidation peak current and  $m$  is the slope of the related calibration curves, were calculated and they were found to be  $7.077 \times 10^{-10}$  mol L<sup>-1</sup> and  $2.35 \times 10^{-9}$  mol L<sup>-1</sup>, respectively. Both LOD and LOQ values confirmed the sensitivity of Met/Pd/CPE/SDS. Intra-day and inter-day ( $n=5$ ) relative standard deviations of samples concentrations (10, 60, and  $100 \times 10^{-6}$  mol L<sup>-1</sup>) of EN were calculated to be 0.04 and 0.06, respectively. Statistical analysis of the results obtained by applying the proposed and the reported methods for the analysis of EN is presented in Table 1.



(Insert Fig. 7)

(insert Table 1)

### 3.6. Simultaneous determination of EN, LD and CD

Combination of EN, LD and CD is used to treat the symptoms of Parkinson's disease and Parkinson's-like symptoms that may develop after encephalitis or injury to the nervous system caused by carbon monoxide poisoning or manganese poisoning. To the best of our knowledge, there is no report on the simultaneous determination of EN, LD, and CD using DPVs. Therefore, the main object of this study was to detect them simultaneously using Met/Pd/CPE/SDS. This was performed by simultaneously changing their concentrations, and recording the DPV. The voltammetric results showed well-defined anodic peaks at potentials of 650, 488 and 320 mV, corresponding to the oxidation of EN, LD, and CD, respectively, indicating that simultaneous determination of these compounds is feasible at Met/Pd/CPE/SDS as shown in Fig. 8.

(Insert Fig 8)

The sensitivity of the modified electrode towards the oxidation of EN was found to be  $0.0504 \mu\text{A}/\mu\text{mol L}^{-1}$ . This is very close to the value obtained in the absence of LD and CD ( $0.0502 \mu\text{A}/\mu\text{mol L}^{-1}$ , see Section 3.5.), indicating that the oxidation processes of these compounds at the Met/Pd/CPE/SDS are independent and therefore, simultaneous determination of their mixtures is possible without significant interferences.

### 3.7. Analytical application

#### 3.7.1. Analysis of Stalevo<sup>®</sup> tablets

The applicability of the proposed electrochemical sensor was checked by analysis of EN in real samples such as pharmaceutical compounds.

Stalevo is a combination with EN, which enhances the bioavailability of CD and LD. Therefore, determination of this drug is very important. The results are given in Table 2, confirm that there are not significant differences between the results of the proposed sensor and the standard method<sup>3</sup>. The results also show that the modified electrode can be used for the determination of EN in real samples with satisfactory results.

(Insert table 2)

### 3.7.2. Validation method in urine

Validation of the procedure for the quantitative assay of EN in urine was examined in B-R buffer pH 2, at scan rate 10 mV/s using DPV. The calibration curve (Fig. 9) gave a straight line in the linear dynamic range  $2 \times 10^{-7} \text{ mol L}^{-1}$  –  $0.4 \times 10^{-4} \text{ mol L}^{-1}$  with correlation coefficient,  $r = 0.9996$ , the LOD is  $1.87 \times 10^{-8} \text{ mol L}^{-1}$  and LOQ is  $6.25 \times 10^{-8} \text{ mol L}^{-1}$ . Four different concentrations on the calibration curve are chosen to be repeated for five times to evaluate the accuracy and precision of the proposed method, which is represented in Table 3. Also, the recovery, standard deviation, standard error and the confidence were calculated.

(Insert table 3)

(Insert Fig. 9)

LOD and LOQ values were compared with values reported by other reported methods for the oxidation of EN at different s, Table 4.

(Insert table 4)

### 3.8. Interferences study

The influence of various substances that potentially interfere with the determination of the studied drugs was studied under optimum conditions using;  $80.0 \times 10^{-3} \text{ mol L}^{-1}$  EN,  $40.0 \times 10^{-3} \text{ mol L}^{-1}$  LD and  $10.0 \times 10^{-3} \text{ mol L}^{-1}$  CD at pH 2.0. The substances that could potentially interfere were chosen from a group of substances commonly found in pharmaceutical preparation; lactose, glucose, cellulose, lactose, sucrose, cross carmellose sodium, starch, colloidal silicon dioxide and magnesium stearate. According to the results, the substances did not interfere, as the tolerance limit was less than  $\pm 5\%$  of the three studied drugs.

### 4. Conclusions

In the present study, carbon paste electrode modified with Met, palladium nanoparticles and SDS was used for the simultaneous determination of EN in the presence of LD and CD. The CV and DPV investigations showed effective electrocatalytic activity, high sensitivity, selectivity, and reproducibility of the voltammetric responses. Very low detection limit, together with the ease of preparation and surface regeneration, make the proposed modified electrode very useful for accurate determination of EN in real samples.

### References

1. Y.-H. Li, T. Wirth, M. Huotari, K. Laitinen, E. MacDonald and P. T. Männistö, *European journal of pharmacology*, 1998, 356, 127-137.
2. D. Nyholm, 2006.
3. C. Paim, H. Gonçalves, A. Lange, D. Miron and M. Steppe, *Analytical Letters*, 2008, 41, 571-581.
4. K. Rajeswari, G. Sankar, A. L. Rao and J. Rao, *International Journal of Chemical Sciences*, 2006, 4, 694-696.

5. C. Paim, H. Gonçalves, D. Miron, J. Sippel and M. Steppe, *Chromatographia*, 2007, 65, 595-599.
6. M. Karlsson and T. Wikberg, *Journal of pharmaceutical and biomedical analysis*, 1992, 10, 593-600.
7. H. Keski-Hynnälä, K. Raanaa, M. Forsberg, P. Männistö, J. Taskinen and R. Kostiainen, *Journal of Chromatography B: Biomedical Sciences and Applications*, 2001, 759, 227-236.
8. N. Ramakrishna, K. Vishwottam, S. Wishu, M. Koteswara and J. Chidambara, *Journal of Chromatography B*, 2005, 823, 189-194.
9. P. Lehtonen, L. Mälkki-Laine and T. Wikberg, *Journal of Chromatography B: Biomedical Sciences and Applications*, 1999, 721, 127-134.
10. H. Keski-Hynnälä, K. Raanaa, J. Taskinen and R. Kostiainen, *Journal of Chromatography B: Biomedical Sciences and Applications*, 2000, 749, 253-263.
11. M. L. Abasq, P. Courtel and G. Burgot, *Analytical Letters*, 2008, 41, 56-65.
12. R. Jain, R. K. Yadav and A. Dwivedi, *Colloids and Surfaces A: Physicochemical and Engineering Aspects*, 2010, 359, 25-30.
13. H. M. Ahmed, M. A. Mohamed and W. M. Salem, *Analytical Methods*, 2015, 7, 581-589.
14. C. Xu, R. Zeng, P. K. Shen and Z. Wei, *Electrochimica acta*, 2005, 51, 1031-1035.
15. N. F. Atta, A. Galal, F. M. Abu-Attia and S. M. Azab, *Journal of the Electrochemical Society*, 2010, 157, F116-F123.
16. N. F. Atta, A. Galal, F. M. Abu-Attia and S. M. Azab, *Journal of Materials Chemistry*, 2011, 21, 13015-13024.

17. B. Rezaei and S. Damiri, *Sensors and Actuators B: Chemical*, 2008, 134, 324-331.
18. J. C. Love, L. A. Estroff, J. K. Kriebel, R. G. Nuzzo and G. M. Whitesides, *Chemical reviews*, 2005, 105, 1103-1170.
19. Q.-M. Xu, L.-J. Wan, C. Wang, C.-L. Bai, Z.-Y. Wang and T. Nozawa, *Langmuir*, 2001, 17, 6203-6206.
20. M. Bhambi, G. Sumana, B. Malhotra and C. Pundir, *Artificial Cells, Blood Substitutes and Biotechnology*, 2010, 38, 178-185.
21. J. Li and X. Lin, *Sensors and Actuators B: Chemical*, 2007, 126, 527-535.
22. M.-P. N. Bui, X.-H. Pham, K. N. Han, C. A. Li, E. K. Lee, H. J. Chang and G. H. Seong, *Electrochemistry Communications*, 2010, 12, 250-253.
23. J. Macanas, L. Ouyang, M. L. Bruening, M. Muñoz, J.-C. Remigy and J.-F. Lahitte, *Catalysis Today*, 2010, 156, 181-186.
24. M. Plavšić, D. Krznarić and B. Ćosović, *Electroanalysis*, 1994, 6, 469-474.
25. S. Guan and B. J. Nelson, *Microelectromechanical Systems, Journal of*, 2006, 15, 330-337.
26. R. Fuchs-Godec, *Colloids and Surfaces A: Physicochemical and Engineering Aspects*, 2006, 280, 130-139.
27. J. Jiang and A. Kucernak, *Journal of Electroanalytical Chemistry*, 2002, 520, 64-70.
28. H. M. Ahmed, M. A. Mohamed and W. M. Salem, *Analytical Methods*, 2015, DOI: 10.1039/C4AY02450H.
29. C. Gouveia-Caridade, R. Pauliukaite and C. Brett, *Electroanalysis*, 2006, 18, 854-861.

30. Y. M. Issa, M. E. Hassoun and A. G. Zayed, *Journal of Liquid Chromatography & Related Technologies*, 2011, 34, 2433-2447.
31. D. B. Gandhi and P. J. Mehta, *JPC-Journal of Planar Chromatography-Modern TLC*, 2011, 24, 236-241.
32. F. Bugamelli, C. Marcheselli, E. Barba and M. Raggi, *Journal of pharmaceutical and biomedical analysis*, 2011, 54, 562-567.
33. N. F. Atta, M. F. El-Kady and A. Galal, *Analytical biochemistry*, 2010, 400, 78-88.
34. M. Mashat, H. Chrystyn, B. J. Clark and K. H. Assi, *Journal of Chromatography B*, 2008, 869, 59-66.
35. N. F. Atta, A. Galal, F. M. Abu-Attia and S. M. Azab, *Electrochimica Acta*, 2011, 56, 2510-2517.
36. <http://www.drugbank.ca/drugs/DB00494>.
37. A. J. Bard and L. R. Faulkner, *Electrochemical methods: fundamentals and applications*, Wiley New York, 1980.
38. A. A. Ensafi, H. Karimi-Maleh, S. Mallakpour and B. Rezaei, *Colloids and Surfaces B: Biointerfaces*, 2011, 87, 480-488.
39. F. El-Taib Heakal, A. Fekry and M. Fatayerji, *Electrochimica Acta*, 2009, 54, 1545-1557.
40. A. Fekry, *Electrochimica Acta*, 2009, 54, 3480-3489.
41. A. Fekry and M. Fatayerji, *Electrochimica Acta*, 2009, 54, 6522-6528.
42. A. Fekry, *international journal of hydrogen energy*, 2010, 35, 12945-12951.
43. J. R. Mcdonald, *Impedance spectroscopy: emphasizing solid materials and systems*, 1987.
44. D. D. Macdonald, *Electrochimica Acta*, 2006, 51, 1376-1388.

45. U. Retter, A. Widmann, K. Siegler and H. Kahlert, *Journal of Electroanalytical Chemistry*, 2003, 546, 87-96.
46. G. Walter, *Corrosion Science*, 1986, 26, 681-703.
47. M. Ameer, *Materials and Corrosion*, 2000, 51, 242-246.
48. R. Vedalakshmi, V. Saraswathy, H.-W. Song and N. Palaniswamy, *Corrosion Science*, 2009, 51, 1299-1307.

**Table 1** Statistical analysis of the results obtained by applying the proposed and the reported methods for the analysis of EN.

| Values          | Proposed method   | Reported method <sup>3</sup> |
|-----------------|-------------------|------------------------------|
| Mean $\pm$ S.D. | 100.16 $\pm$ 0.55 | 99.11 $\pm$ .98              |
| n               | 5                 | 5                            |
| Variance        | 0.30              | 0.96                         |
| t (2.776)       | 2.1               | -----                        |
| F(6.390)        | 3.2               | -----                        |

\*Values between parentheses are the theoretical values of t and F at confidence 95%.

**Table 2** Application of the proposed method to determination of EN in its pharmaceutical preparation Stalevo<sup>®</sup>.

| Proposed voltammetric method |   |   |                  |
|------------------------------|---|---|------------------|
| Parameters                   | Taken<br>10 <sup>-6</sup> mol L <sup>-1</sup> | Found<br>10 <sup>-6</sup> mol L <sup>-1</sup> | Recovery*%       |
| EN                           | 20.00   | 19.65   | 98.25            |
|                              | 60.00   | 61.00   | 101.66           |
|                              | 100.00  | 98.00   | 98.00            |
| Mean $\pm$ S.D.              |   |   | 99.30 $\pm$ 1.44 |
| LD                           | 10.00   | 10.00   | 100.00           |
|                              | 30.00   | 30.06   | 100.20           |
|                              | 50.00   | 49.88   | 99.76            |
| Mean $\pm$ S.D.              |   |   | 99.90 $\pm$ 0.26 |
| CD                           | 2.50  | 2.49  | 99.60            |
|                              | 7.50  | 7.48  | 99.73            |
|                              | 12.50   | 12.51   | 100.08           |
| Mean $\pm$ S.D.              |   |   | 99.80 $\pm$ 0.25 |

\*Average of three determinations.



**Table 3** Accuracy and precision of the proposed method in urine

| C.L. <sup>c</sup> x10 <sup>-6</sup> | S.E <sup>b</sup> x10 <sup>-7</sup> | SDx10 <sup>-7</sup> | Recovery(%) | [EN]<br>Found <sup>a</sup><br>( $\mu\text{mol L}^{-1}$ ) | [EN]<br>added<br>( $\mu\text{mol L}^{-1}$ ) |
|-------------------------------------|------------------------------------|---------------------|-------------|--|---|
| 0.08                                | 0.27                               | 0.55                | 99.88       | 24.97  | 25.00                                       |
| 0.39                                | 1.25                               | 2.50                | 100.1       | 75.07  | 75.00                                       |
| 1.39                                | 4.11                               | 8.22                | 99.96       | 149.9  | 150.0                                       |
| 0.16                                | 0.50                               | 1.01                | 99.97       | 299.9  | 300.0                                       |

<sup>a</sup> mean for five determinations

<sup>b</sup>Standard error =  $SD/\sqrt{n}$

<sup>c</sup>C.L. confidence at 95%confidence level and 4 degrees of freedom ( $t=2.776$ )

**Table 4** Comparison of the proposed electrochemical sensor with the reported method for the determination of EN

| Ref.          | LDR<br>( $\text{mol L}^{-1}$ )                   | LOD<br>( $\text{mol L}^{-1}$ ) | pH  | Method | Modifier                                   | Electrode                                   |
|---------------|--|--------------------------------|-----|--------|--|---|
| <sup>11</sup> | $1.50 \times 10^{-4}$ -<br>$3.50 \times 10^{-4}$ | $1.41 \times 10^{-4}$          | 2.3 | DPVs   | -----                                      | Dropping<br>Mercury<br>Electrode            |
| <sup>12</sup> | $5 \times 10^{-4}$ - $1.8 \times 10^{-5}$        | $3.95 \times 10^{-8}$          | 2.5 | SWV    | Tween 20                                   | Hanging<br>mercury<br>dropping<br>electrode |
| This<br>work  | $2.0 \times 10^{-8}$ - $0.8$<br>$\times 10^{-3}$ | $7.077 \times 10^{-10}$        | 2   | DPVs   | Pd<br>nanoparticles,<br>Methionine,<br>SDS | Carbon paste                                |

**List of figures**

Scheme 1 Structures of EN (A), LD (B) and CD (C).

Scheme 2 The suggested oxidation mechanism of EN at Met/Pd/CPE/SDS.

**Fig. 1** Scanning electron microscope image of A) bare CPE, B) Met/CPE and C) Met/Pd/CPE.

**Fig. 2** Cyclic voltammograms of  $1.0 \times 10^{-3} \text{ mol L}^{-1}$  EN in B-R buffer pH 2 at a scan rate of  $100 \text{ mV s}^{-1}$  recorded at four different working electrodes.

**Fig. 3** Cyclic voltammetric response of  $1.0 \times 10^{-3} \text{ mol L}^{-1}$  EN at different pH values using Met/Pd/CPE/SDS.

The inset: plot of the anodic peak current values of EN versus pH values using different electrodes.

**Fig. 4** The effect of different scan rates (from 10 to  $100 \text{ mVs}^{-1}$ ) on the current response of EN ( $1.0 \times 10^{-3} \text{ mol L}^{-1}$ ) using Met/Pd/CPE/SDS in B-R buffer (pH 2).

The inset: relation between the anodic peak currents of EN with increasing the scan rate.

**Fig. 5** (A) Chronoamperograms obtained at Met/Pd/CPE/SDS in B-R buffer (pH 2) for different concentration of EN. The numbers 1–6 correspond to 2.5, 5.0, 12.5, 25.0, 50.0 and  $62.5 \mu\text{mol L}^{-1}$  of EN. Insets: (A) Plots of  $I$  vs.  $t^{1/2}$  obtained from chronoamperograms 1–6. (B) Plot of the slope of the straight lines against EN concentration.

**Fig. 6A** The Bode plots of EIS scans of bare CPE, Met/CPE, Met/Pd/CPE and Met/Pd/CPE/SDS. Inset: Equivalent circuit used in the fit procedure of the impedance spectra.

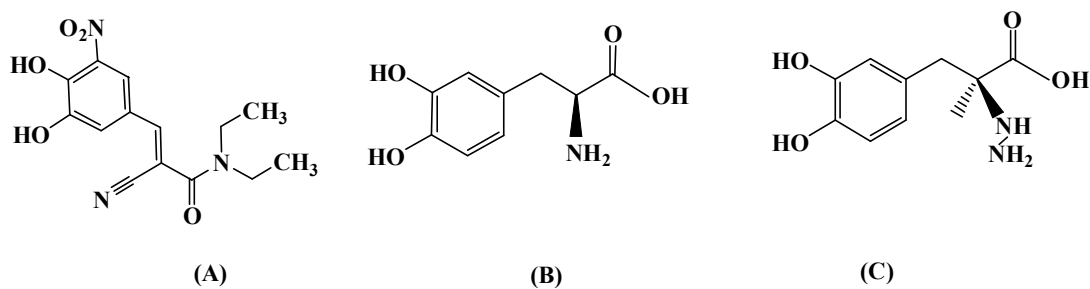
**Fig. 6B** The Nyquist plots of EIS scans of bare CPE and Met/CPE, Inset: The Nyquist plots of EIS scans of Met/Pd/CPE and Met/Pd/CPE/SDS.

**Fig. 7** The effect of changing the concentration of EN, using differential pulse mode at Met/Pd/CPE/SDS in  $0.04 \text{ mol L}^{-1}$  B-R buffer pH 2 and scan rate  $10 \text{ mV s}^{-1}$ .

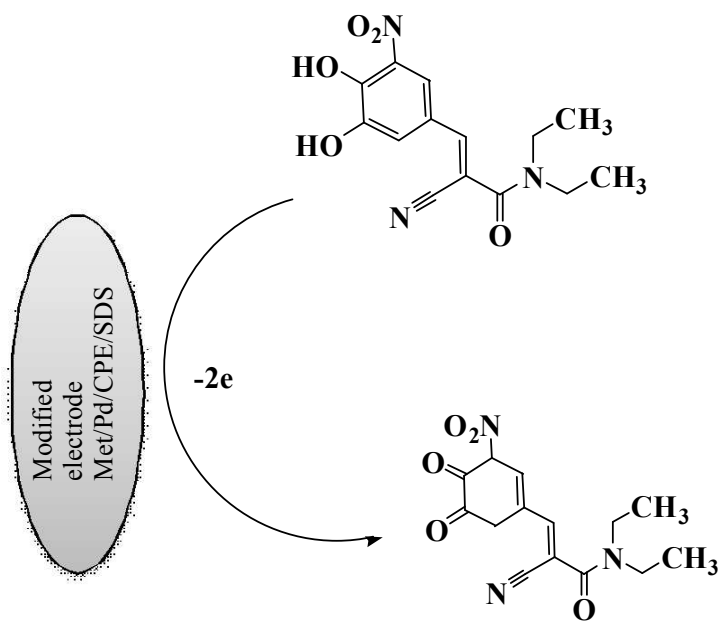
The inset: The calibration plot of EN.

**Fig. 8** DPVs of Met/Pd/CPE/SDS in B-R buffer (pH 2) containing different concentrations of EN from inner to outer: 99, 129, 177, 197, 394 and  $620 \mu\text{mol L}^{-1}$  in the presence of CD ( $2.50 \times 10^{-3} \text{ mol L}^{-1}$ ) and LD ( $10 \times 10^{-3} \text{ mol L}^{-1}$ ) at scan rate  $10 \text{ mV/s}$ . Inset shows the plot of the peak current as a function of EN concentration

**Fig. 9** Calibration plot of EN in urine, using differential pulse mode at Met/Pd/CPE/SDS in  $0.04 \text{ mol L}^{-1}$  B-R buffer pH 2 and scan rate  $10 \text{ mV s}^{-1}$ .



**Scheme 1** Structures of EN (A), LD (B) and CD (C).



**Scheme 2** The suggested oxidation mechanism of EN at Met/Pd/CPE/SDS.

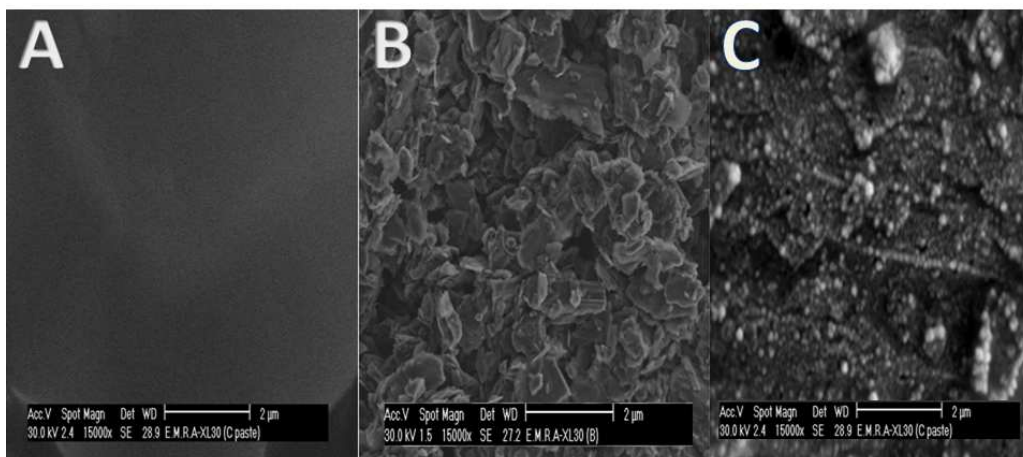


**Fig. 1** Scanning electron microscope image of A) bare CPE, B) Met/CPE and C) Met/Pd/CPE.

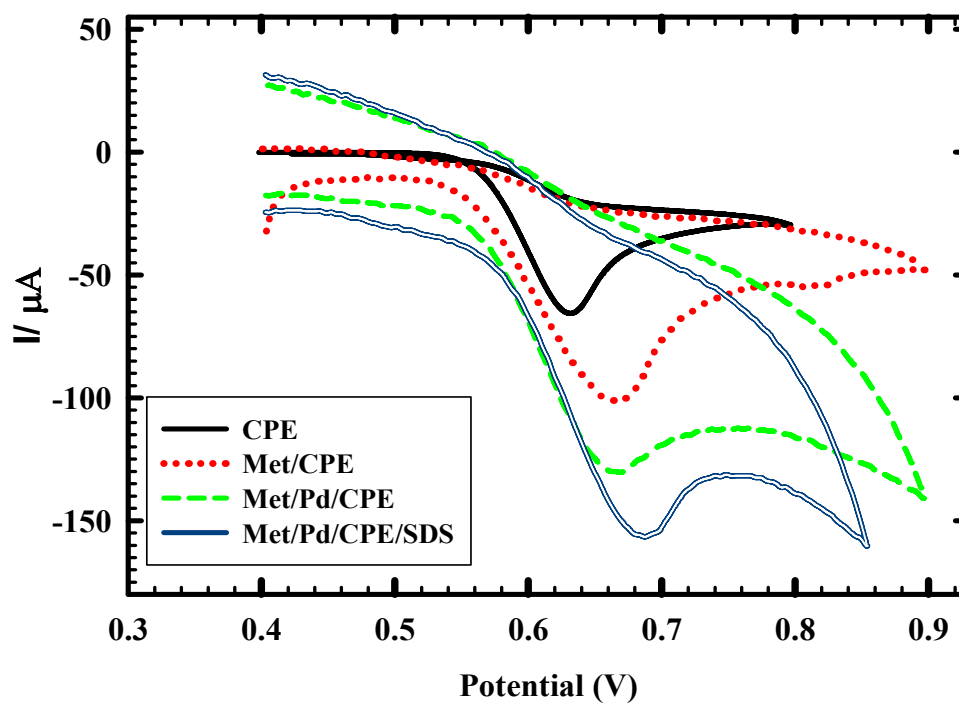


**Fig. 2** Cyclic voltammograms of  $1.0 \times 10^{-3} \text{ mol L}^{-1}$  EN in B-R buffer pH 2 at a scan rate of  $100 \text{ mV s}^{-1}$  recorded at four different working electrodes.

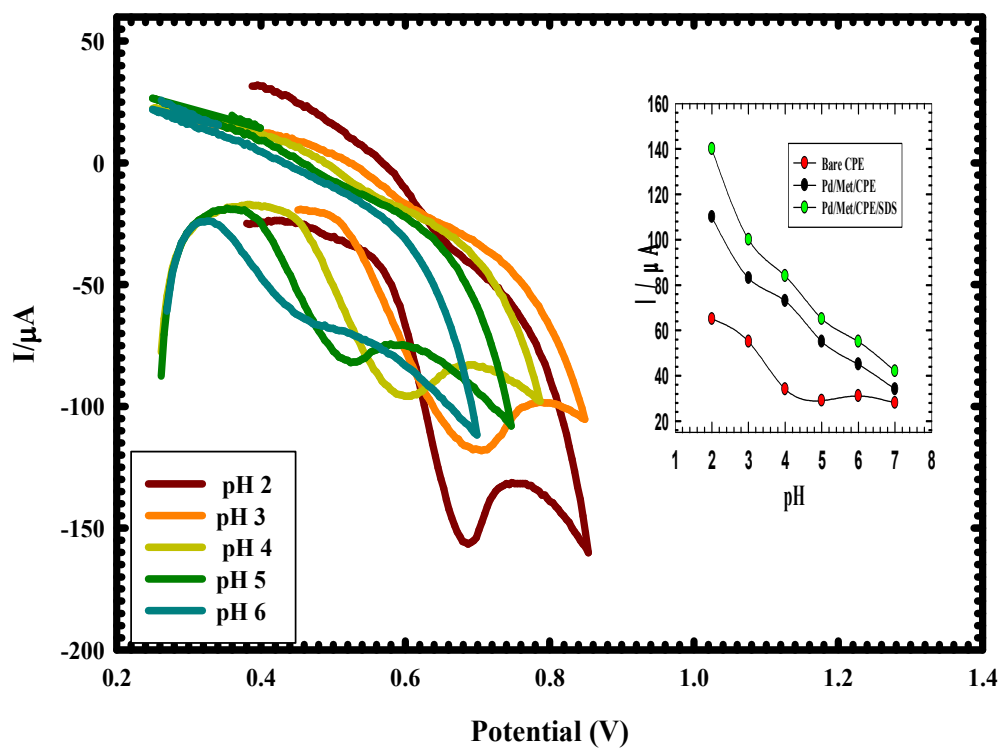


**Fig. 3** Cyclic voltammetric response of  $1.0 \times 10^{-3} \text{ mol L}^{-1}$  EN at different pH values using Met/Pd/CPE/SDS.

The inset: plot of the anodic peak current values of EN versus pH values using different electrodes.

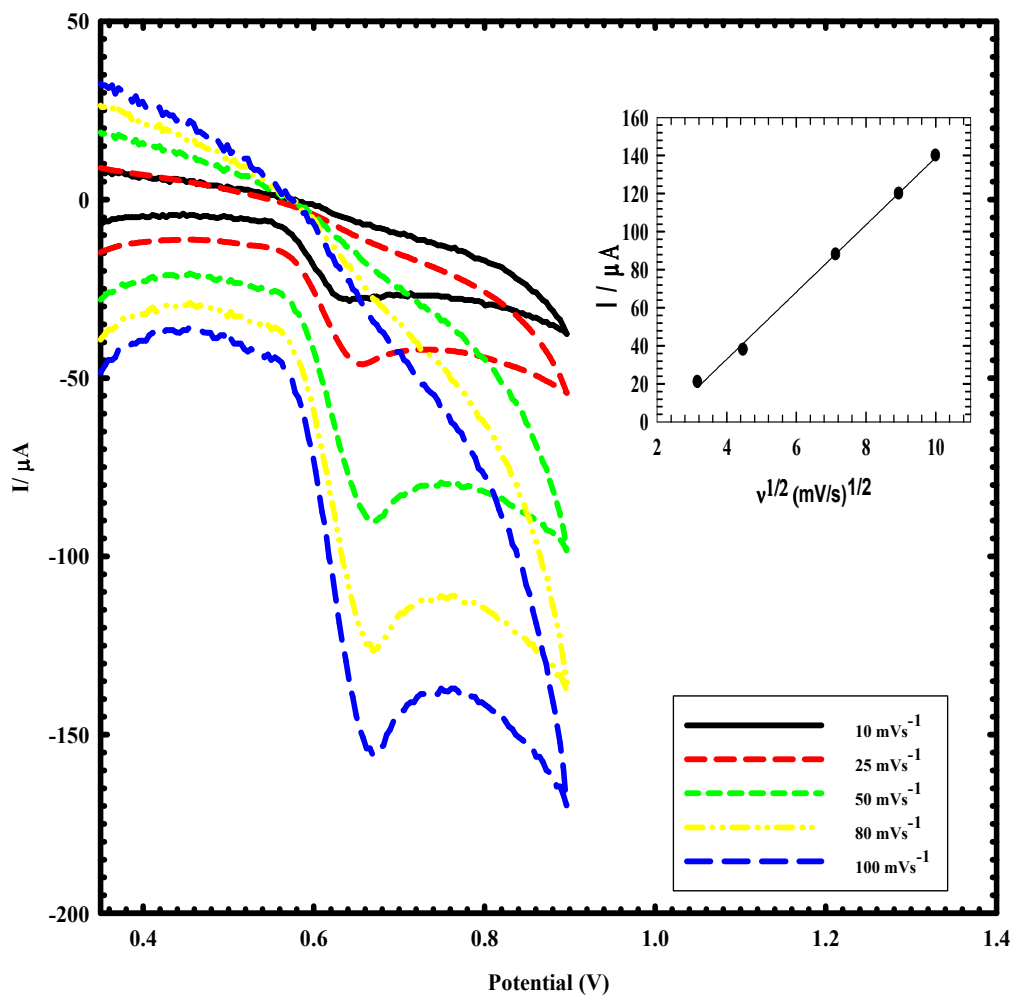


**Fig. 4** The effect of different scan rates (from 10 to 100  $\text{mVs}^{-1}$ ) on the current response of EN ( $1.0 \times 10^{-3} \text{ mol L}^{-1}$ ) using Met/Pd/CPE/SDS in B-R buffer (pH 2).

The inset: relation between the anodic peak currents of EN with increasing the scan rate.

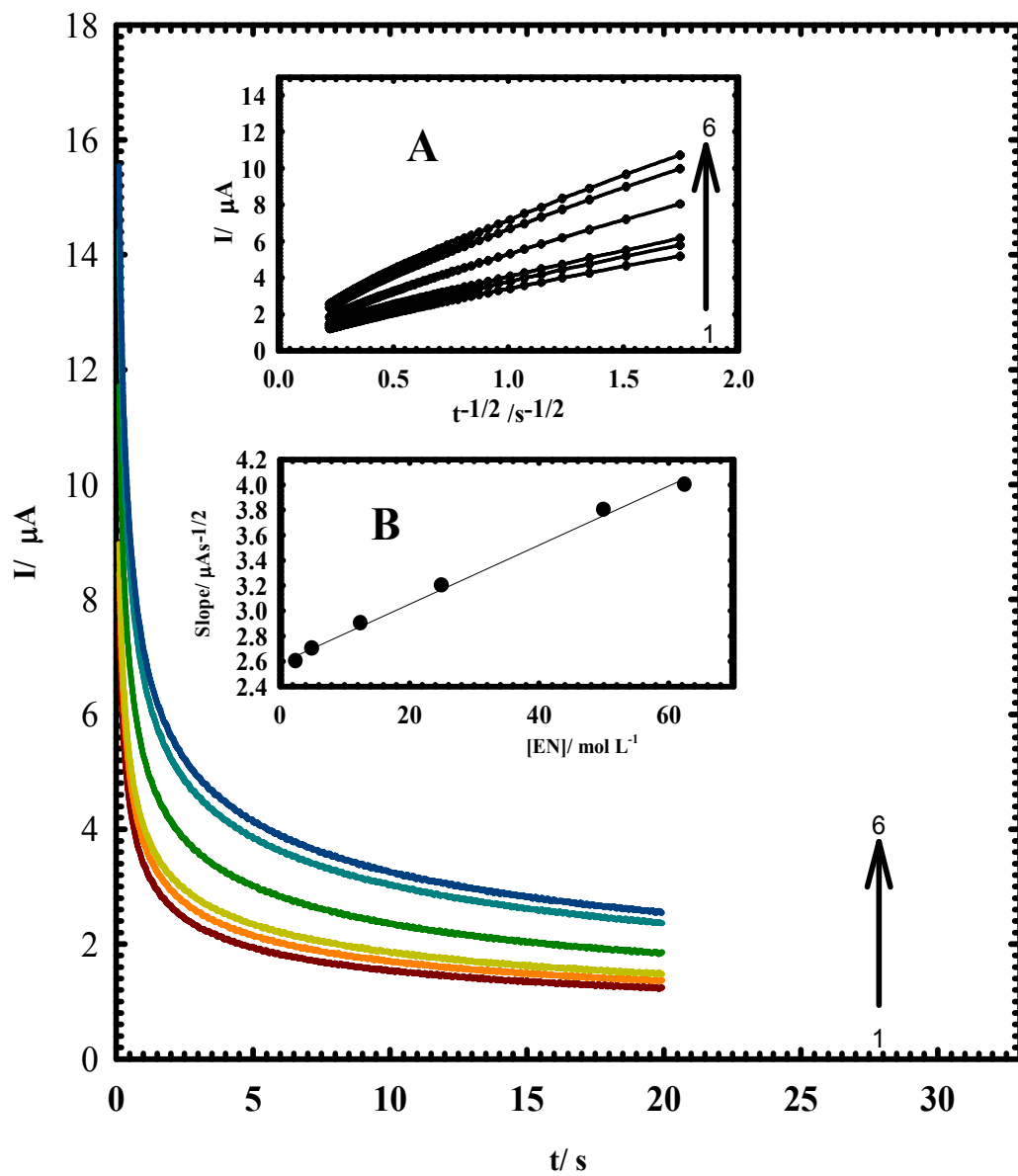


**Fig. 5** (A) Chronoamperograms obtained at Met/Pd/CPE/SDS in B-R buffer (pH 2) for different concentration of EN. The numbers 1–6 correspond to 2.5, 5.0, 12.5, 25.0, 50.0 and 62.5  $\mu\text{mol L}^{-1}$  of EN. Insets: (A) Plots of  $I$  vs.  $t^{-1/2}$  obtained from chronoamperograms 1–6. (B) Plot of the slope of the straight lines against EN concentration.



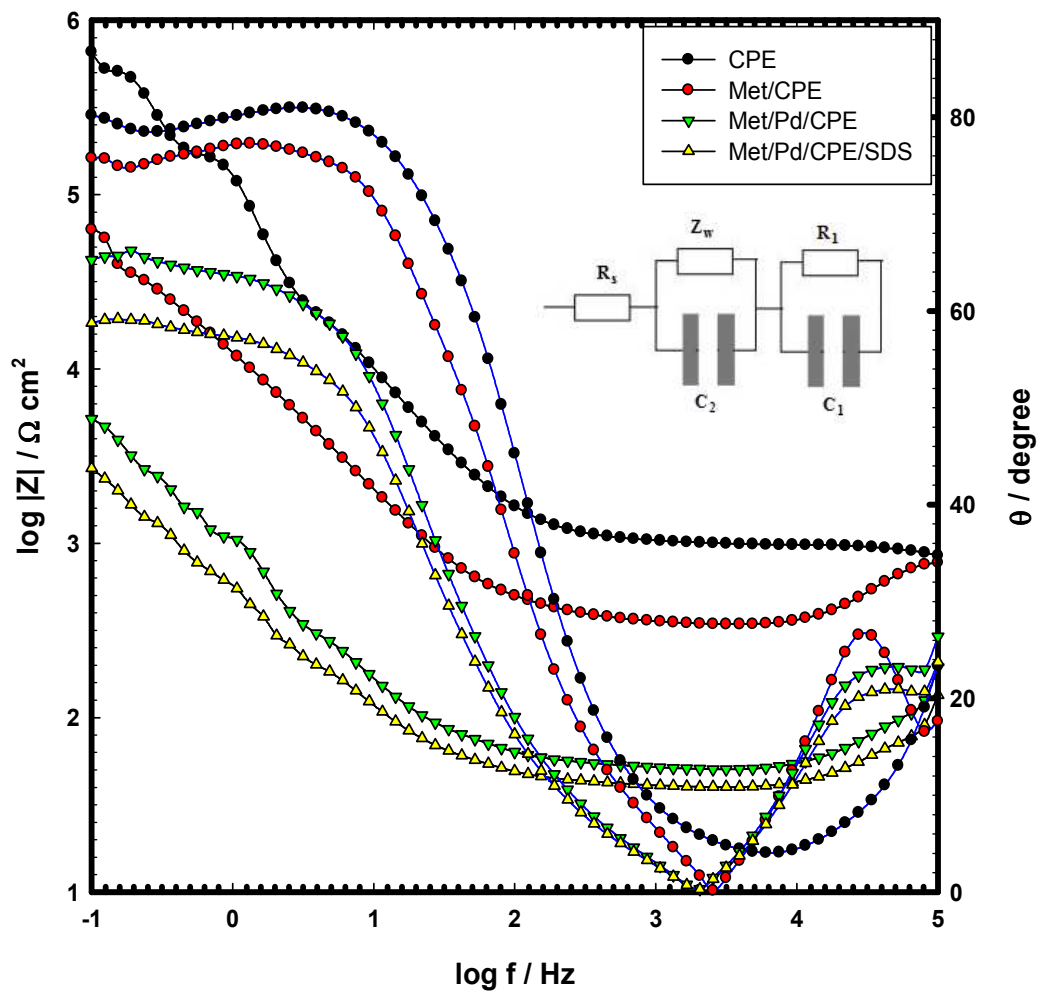


**Fig. 6A** The Bode plots of EIS scans of bare CPE, Met/CPE, Met/Pd/CPE and Met/Pd/CPE/SDS. Inset: Equivalent circuit used in the fit procedure of the impedance spectra.

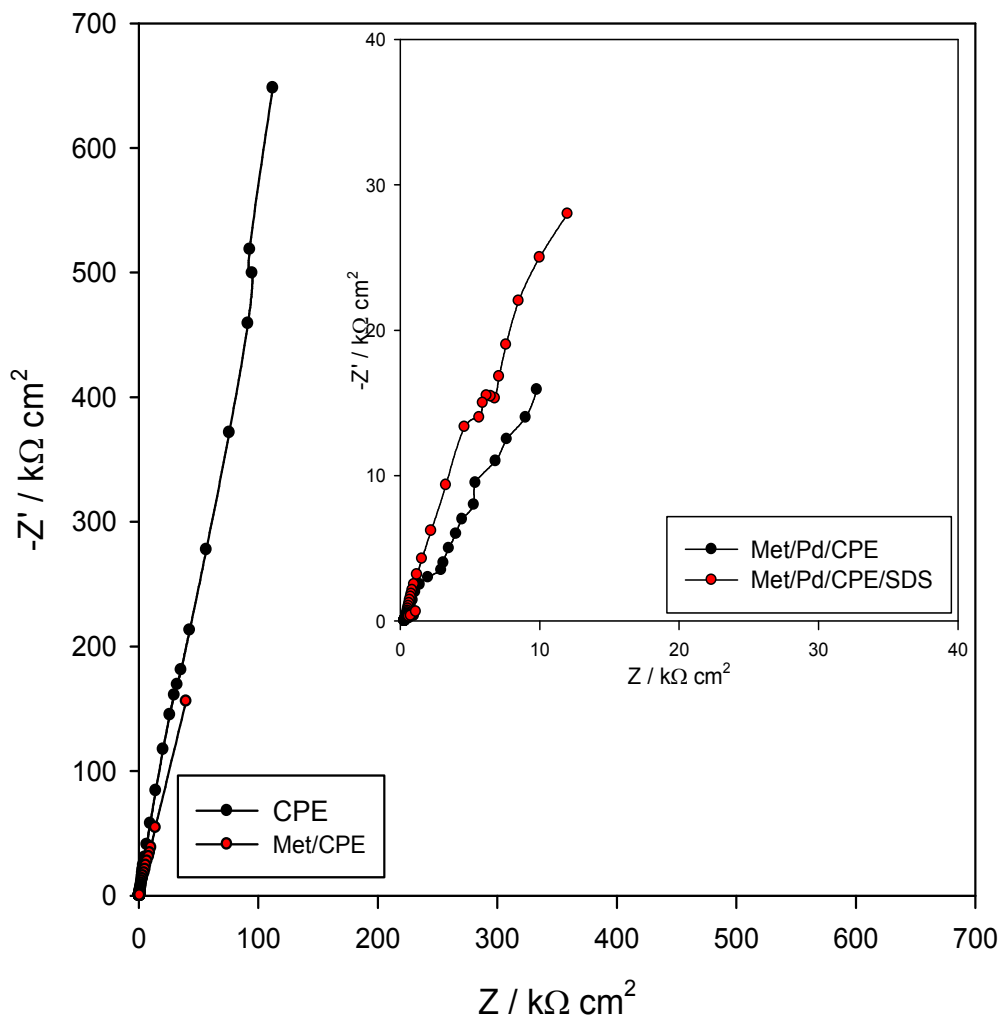


**Fig. 6B** The Nyquist plots of EIS scans of bare CPE and Met/CPE, Inset: The Nyquist plots of EIS scans of Met/Pd/CPE and Met/Pd/CPE/SDS.

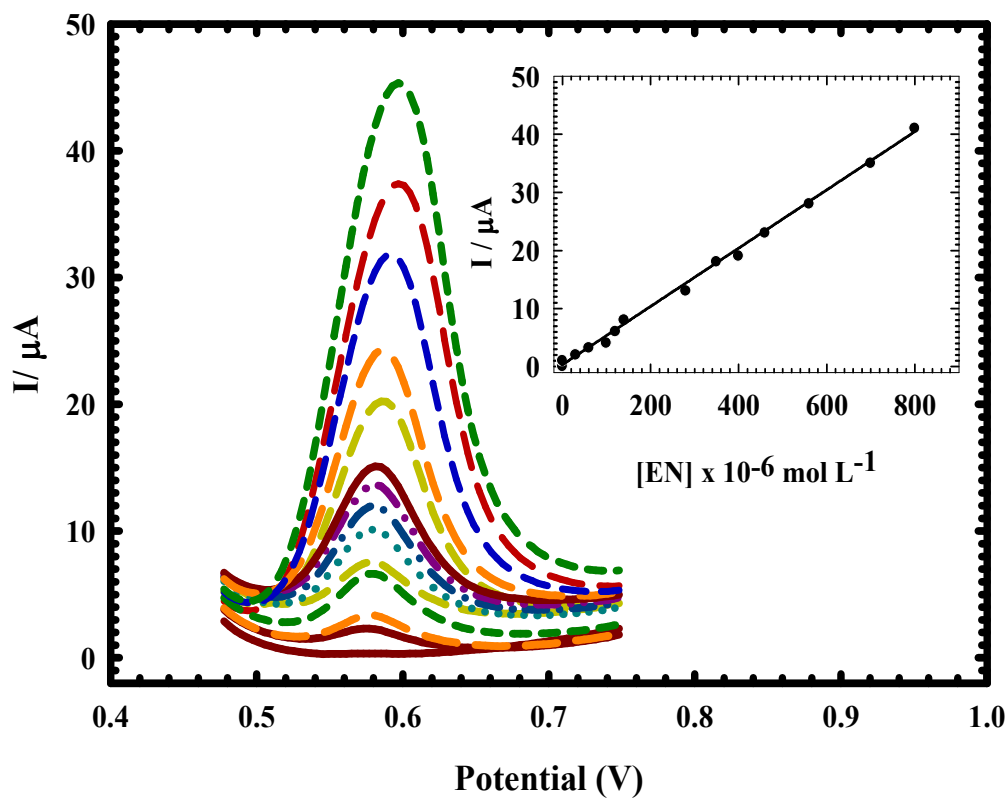


**Fig. 7** The effect of changing the concentration of EN, using differential pulse mode at Met/Pd/CPE/SDS in  $0.04 \text{ mol L}^{-1}$  B-R buffer pH 2 and scan rate  $10 \text{ mV s}^{-1}$ .

The inset: The calibration plot of EN.

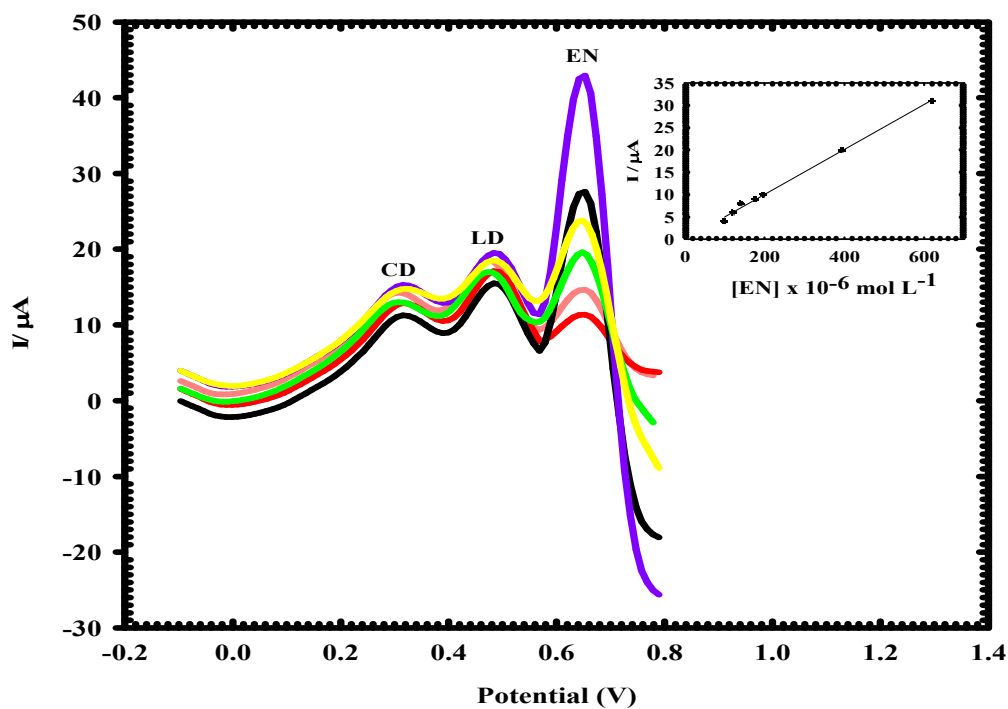


**Fig. 8** DPVs of Met/Pd/CPE/SDS in B-R buffer (pH 2) containing different concentrations of EN from inner to outer: 99, 129, 177, 197, 394 and 620  $\mu\text{mol L}^{-1}$  in the presence of CD ( $2.50 \times 10^{-3} \text{ mol L}^{-1}$ ) and LD ( $10 \times 10^{-3} \text{ mol L}^{-1}$ ) at scan rate 10 mV/s. Inset shows the plot of the peak current as a function of EN concentration

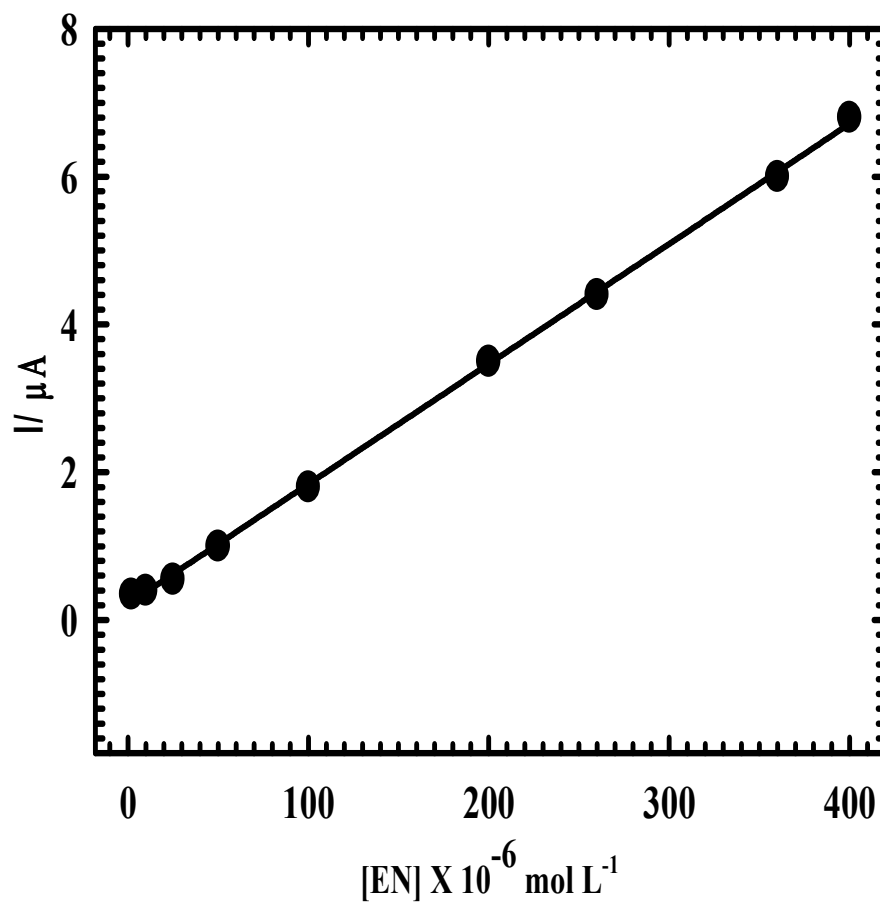


**Fig. 9** Calibration plot of EN in urine, using differential pulse mode at Met/Pd/CPE/SDS in  $0.04 \text{ mol L}^{-1}$  B-R buffer pH 2 and scan rate  $10 \text{ mV s}^{-1}$ .

